RADIOFREQUENCY SPECTROSCOPY OF STORED IONS I: STORAGE*

H. G. DEHMELT

Department of Physics, University of Washington
Seattle, Washington

1. Introduction

Experimental attempts to approach the ideal of isolated atomic systems floating at rest in free space for unlimited periods and free from any undesired outside perturbations appear to be worthwhile for a variety of reasons. At the same time such experiments are of limited value unless one also devises means for first preparing the atomic systems in certain selected states and for later observing the development of these states in time due to internal or controlled external interactions, as in a hfs or magnetic resonance experiment. The first experimental goal therefore is to develop techniques to isolate, contain in a trap, thermalize, and possibly refrigerate the atomic systems under study. Since these problems appear to be most easily solved for charged particles, we restrict ourselves in the following to ions. Next, collision reactions with suitable, state-selected projectiles may serve to create oriented, aligned, or somehow state-selected ions from atoms or cause ions already present in the trap to undergo transitions to selected states. A second reaction, not

* Part II: Spectroscopy is now scheduled to appear in Volume V of this series.

necessarily of the same type, may be used for analysis or interrogation of the stored ions. A whole arsenal of suitable projectiles becomes available once ion containment times of sufficient duration, of the order of seconds, are realized, bringing down the necessary projectile flux densities to feasible values. General discussions of the subject have been given by the author who also previously suggested rf spectroscopy of stored ions (Dehmelt, 1956a, 1962, 1963). An experiment (Dehmelt and Major, 1962; Major, 1962; Major and Dehmelt, 1967) carried out on He^+ ions with the intent of observing their magnetic resonance may serve as an illustrative example; He^+ ions contained under ultrahigh vacuum conditions in an electric quadrupole rf trap (Paul *et al.*, 1958; Fischer, 1959; Wuerker *et al.*, 1959) were bombarded with polarized Cs atoms. In the ensuing spin-exchange collisions, the He^+ electron spins became oriented according to the reactions

$$Cs\uparrow + He^+\uparrow \rightarrow Cs\uparrow + He^+\uparrow \quad \text{and} \quad Cs\uparrow + He^+\downarrow \rightarrow Cs\downarrow + He^+\uparrow \tag{1.1}$$

while the Cs atoms lost orientation. This experiment is closely related to an earlier experiment (Dehmelt, 1956b, 1958a,b; Balling and Pipkin, 1965) in which free electrons contained by a positive ion cloud were oriented by spin-exchange collision with oriented sodium atoms,

$$Na\uparrow + e\uparrow \rightarrow Na\uparrow + e\uparrow \quad \text{and} \quad Na\uparrow + e\downarrow \rightarrow Na\downarrow + e\uparrow. \tag{1.2}$$

In both instances, magnetic resonance disorientation of the ions He^+ and e, the process of interest, was monitored by a second collision reaction. In general, information about the magnetic resonance is contained in the final states of all the reaction products. In the electron experiment the monitoring focused on the orientation loss of the sodium atoms or of the "projectiles." Since spin-exchange reactions between oriented electrons e↑ and Na↑ atoms do not produce Na↓ atoms while e↓, Na↑ collisions do, the appearance of Na↓ did serve as an indicator for the magnetic resonance disorientation of the electrons. In the He^+ experiments the orientation monitoring phase focused upon the He^+ targets and not the Cs↑ projectiles. By employing the nearly resonant charge-exchange reaction leading to excited He states,

$$\begin{aligned} Cs\uparrow + He^+\downarrow &\xrightarrow{\text{fast}} Cs^+ + He^* \quad \text{(singlet)}, \\ Cs\uparrow + He^+\uparrow &\xrightarrow{\text{slow}} Cs^+ + He^* \quad \text{(triplet)}, \end{aligned} \tag{1.3}$$

it was possible to translate the magnetic resonance disorientation of the initially oriented $He^+\uparrow$ ions to $He^+\downarrow$ into a reduction of their number, which in turn could be conveniently measured. The appearance of a new reaction product, namely, Cs^+, might have provided an even more effective indicator of the He^+ resonance. In fact, in a third experiment on H_2^+ ions (Dehmelt and Jefferts, 1962; Jefferts, 1962; Richardson *et al.*, 1967), using linearly polarized photons as projectiles in the dissociation reaction

$$h\nu\,\updownarrow + H_2^+\,\updownarrow \rightarrow H^+ + H + \text{K.E.}, \qquad h\nu\,\updownarrow + H_2^+ \multimap\!\!\leftrightarrow H^+ + H + \text{K.E.}, \tag{1.4}$$

the appearance of H^+ was used to monitor the magnetic resonance of H_2^+. This again is possible because the photodissociation rate depends on the angle between electric light vector ↕ and the internuclear axis ↕. As illustrated by the three experiments just described, our studies seem to indicate that a wide variety of target-projectile combinations of interest may be imagined. The state selection of the projectiles necessary may be purely by energy eigenstate, as low as that found in an unpolarized monoenergetic parallel beam of electrons (alignment by electron impact), or as high as that in a beam of circular polarized optical resonance radiation (optical pumping), or in a beam of polarized alkali atoms (polarization by spin exchange). The ion-storage collision technique outlined has now been applied successfully to a precise determination of the hfs separation of the hydrogen-like $(He^3)^+$ ion in the 8-GHz region (Fortson *et al.*, 1966) and to the first study of the Zeeman effect in H_2^+ yielding a value for the spin-rotational coupling constant.

2. Containment of Isolated Ions

2.1. Limitations

Having stated our experimental goal, we shall briefly touch upon some fundamental and technical limitations before discussing specific containment methods. It is, of course, impossible in principle to have a confined particle totally at rest. Rather, when for reasons of Doppler effect suppression (Dicke, 1953) it is necessary to restrict a particle to a region smaller than a quarter wavelength $\lambda/4$ of the microwave spectrum to be studied, its de Broglie wavelength λ_B must always be shorter than $\lambda/2$. Evaluating the velocity of a proton with $\lambda_B = 0.1$ cm as an illustration, we find $v \simeq 4 \times 10^{-2}$ cm/sec. On a temperature scale this amounts to only about 6×10^{-12}°K, a negligible value. We would like to be sure that the relatively long-range forces between the slow ion of interest and the unavoidable background gas atoms do not in practice lead to an excessively short mean time T_r between collisions. From Langevin's analysis (Stevenson and Gioumousis, 1958) of orbiting collisions leading to an inward spiraling orbit and close contact, we obtain

$$T_r = (m_r/\alpha_r)^{1/2}/(2\pi e n_r) \tag{2.1}$$

in the limit of a stationary ion, where n_r, α_r, and m_r are density, polarizability, and mass of the residual gas atoms and e is the charge on the ion. Taking He as the residual gas at the technically feasible pressure of $\sim 10^{-13}$ Torr, we find the very large value $T_r \simeq 10^7$ sec independent of the kinetic energy of the gas atom, K_r. The closest approach r_e for excluded, nonorbiting encounters is here given by

$$r_e^4 = \tfrac{1}{2}\alpha_r e^2/K_r. \tag{2.2}$$

For He at room temperature impinging upon a singly charged stationary ion this gives $r_e \simeq 2.5 \times 10^{-8}$ cm, a value which is somewhat enlarged by cooling. (Throughout the article cgs units have been used unless other units are specified.) After this illustration of the degree of isolation now within the state of the art we will turn to a review of the principal containment methods useful in rf spectroscopy.

2.2. Penning Trap

Even though this scheme does not strictly belong to those admissible under our title, we will begin with a discussion of the Penning arrangement which we are using for the containment of electrons as well as cyclotron resonance and thermalization studies of these particles (Dehmelt, 1961). The confinement mechanism is that of the Penning discharge widely used in cold cathode ionization gages and ion-getter pumps. In our embodiment of this principle (Penning, 1936; Pierce, 1949) hyperbolic electrodes (see Fig. 1) create a dc electric potential of the form

$$\phi(x, y, z) = A(x^2 + y^2 - 2z^2), \qquad A = A_0 = \text{const}, \tag{2.3}$$

while a homogeneous magnetic field H_0 points in the z direction. The quantity A_0 is related to $D \equiv \phi(0, 0, 0) - \phi(0, 0, z_0)$, the depth of the potential well in the z direction, by $D = 2z_0^2 A_0$. We also have

$$U = U_0 = D[1 + \tfrac{1}{2}(r_0/z_0)^2] > 0,$$

U being the applied voltage. The electrons move along bound orbits which are characterized by three frequencies. An electron moving along the z axis sees a parabolic potential and will undergo harmonic oscillations with a frequency ω_z,

$$\omega_z^2 = 4eA_0/m. \tag{2.4}$$

Another simple type of orbit is a circle in the x-y plane with center at the origin. For these orbits the electric force $-eE_r$ almost balances the magnetic force $-e(v/c)H_0$. The frequency of this magnetron motion is a constant of the trap:

$$\omega_m = v/r = cE_r/(H_0 r) = 2cA_0/H_0. \tag{2.5}$$

The third frequency is the cyclotron frequency ω_c given by

$$\omega_c \equiv eH_0/(mc). \tag{2.6}$$

For the particular values of parameters of experimental interest to us, the orbits in general are approximately a superposition of a fast, small-diameter cyclotron motion around a magnetic field line, an oscillation along this field

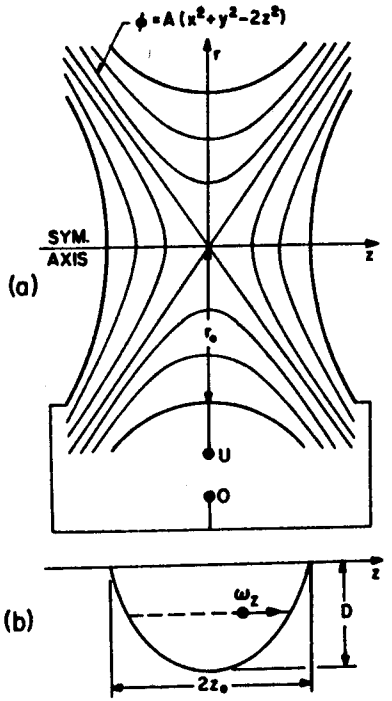

Fig. 1. Hyperbolic electrode configuration employed in ion storage devices useful in rf spectroscopy. Application of an alternating voltage $U = V_0 \cos \Omega t$ at the terminals shown in (a) creates a three-dimensional harmonic oscillator potential of depth $D = D$ along the z axis as depicted in (b). When a dc voltage $U = U_0$ is applied the potential at the origin has a saddle point only. While a parabolic well is also obtained along the z axis, motion of the charged particles in the r direction has to be restricted in this embodiment of the Penning discharge geometry by a strong axial magnetic field as usual.

line, and a slow circular drift across the field lines around the z axis, with respective frequencies $\omega_c \gg \omega_z \gg \omega_m$. From the foregoing we see that these quantities are related by

$$2\omega_c \omega_m = \omega_z^2. \tag{2.7}$$

A more accurate analysis shows that the frequencies of cyclotron and magnetron motion are slightly shifted to $\omega_c - \omega_m'$ and ω_m'. Relation (2.7) is replaced by

$$2\omega_c \omega_m' - 2\omega_m'^2 = \omega_z^2. \tag{2.8}$$

The trap is filled by shooting through it, along the z axis, a narrow electron beam of an energy sufficient to ionize the residual gas. In ultrahigh vacuums a beam of low energy electrons is reflected upon itself. Temporary trapping

occurs by transformation of longitudinal kinetic energy into transverse due to e-e collisions. By providing simultaneously a radiative damping mechanism the trapping is made permanent. In experiments carried out by Walls, trapping times of hours have been realized for about 10^4 electrons in the trap at a background pressure of 2×10^{-11} Torr. The trap parameters are listed in Table I. Compare also Fig. 1.

TABLE I

OPERATING PARAMETERS OF PENNING TRAP FOR CONTAINMENT OF THERMAL ELECTRONS

Electrode dimensions:	$2z_0 = 1$ cm, $r_0/z_0 = \sqrt{2}$
Magnetic field:	$H_0 = 7.8$ kG
dc operating voltage:	$U_0 = 2D = 12.8$ volts
Cyclotron frequency:	$\omega_c/(2\pi) = 22.4$ GHz
Axial oscillation frequency:	$\omega_z/(2\pi) = 58$ MHz
Magnetron (drift) frequency:	$\omega_m/(2\pi) = 75$ kHz

2.3. AVERAGE FORCE IN INHOMOGENEOUS rf FIELD

The obvious shortcoming of the type of trap just described is the presence of the magnetic field, causing a large and often undesired Zeeman effect. This difficulty does not arise in the trap design based on the use of inhomogeneous electric rf fields (Paul *et al.*, 1958; Fischer, 1959; Wuerker *et al.*, 1959). The related mass-filter (Paul and Steinwedel, 1953) is now widely used in the commercial quadrupole residual gas analyzers. To illustrate it we first consider an ion of charge e and mass m moving in the homogeneous electric rf field of a parallel plate capacitor [see Fig. 2(a)]. The equation of motion is

$$m\ddot{z} = F_z(t) = eE_0 \cos \Omega t, \qquad E_0 = V_0/(2z_0). \tag{2.9}$$

We seek a solution of the form $z(t) = \bar{z} + \zeta(t)$, $\bar{z} = \text{const}$, and obtain

$$\zeta = -\zeta_0 \cos \Omega t, \qquad \zeta_0 = eE_0(z)/(m\Omega^2). \tag{2.10}$$

The time variation of the force $F_z(t) = eE_0 \cos \Omega t$ and the coordinate z are depicted in Figs. 2(b) and 2(c). Making the field inhomogeneous, as in the modified geometry indicated by broken lines, without changing its value at $\bar{z}$, slightly perturbs the orbit [now $\zeta'(t)$] of and the force [now $F_z'(t)$] acting on the ion. The interesting net effect is that the time average of the alternating force, $\langle F_z'(t) \rangle_{av}$, is now finite,

$$\bar{F}(\bar{z}) \equiv \langle F_z'(t) \rangle_{av} = \langle eE_0(z(t)) \cos \Omega t \rangle_{av}$$

though small compared to its maximum value. The direction of $\bar{F}(\bar{z})$ is toward the region of weaker field. For a quantitative evaluation of $\bar{F}(\bar{z})$ in the limit of very large Ω we imagine it balanced, so that the center of the sinusoidal micromotion at frequency Ω remains at rest at $\bar{z}$. We expand $E_0(z)$ around $\bar{z}$,

$$E_0(z) = E_0(\bar{z}) + [\partial E_0(\bar{z})/\partial \bar{z}]\zeta, \qquad |[\partial E_0(\bar{z})/\partial \bar{z}]\zeta_0| \ll |E_0(\bar{z})|.$$

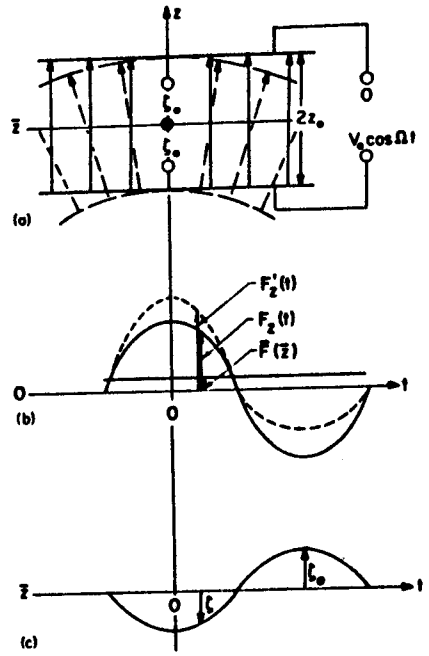

FIG. 2. Principle of rf electric quadrupole ion cage. While the force $F_z(t)$ causing the micromotion displacement ζ of an ion from its guiding center $\bar{z}$ has a vanishing time average for a homogeneous rf field (full lines) this is no longer the case in an inhomogeneous field of the same intensity (broken lines). Here the averaging of the modified instantaneous force $F_z'(t)$ over the essentially unaltered micromotion $\zeta(t)$ leads to a small, nonvanishing average force $\bar{F}(\bar{z})$, which always points toward the region of weaker rf fields independent of the sign of the ionic charge.

Averaging over one period, we may write

$$\begin{aligned}(1/e)\bar{F}(\bar{z}) &= \langle E_0(\bar{z}) \cos \Omega t + [\partial E_0(\bar{z})/\partial \bar{z}]\zeta' \cos \Omega t \rangle_{av} \\ &= [\partial E_0(\bar{z})/\partial \bar{z}]\langle \zeta' \cos \Omega t \rangle_{av}.\end{aligned} \tag{2.11}$$

For ζ' the expression (2.10) for ζ may be used in excellent approximation:

$$\langle \zeta' \cos \Omega t \rangle_{av} = -\tfrac{1}{2}\zeta_0 = -eE_0(\bar{z})/(2m\Omega^2).$$

Finally, we have

$$(1/e)\bar{F}(\bar{z}) = -e[\partial E_0(\bar{z})/\partial\bar{z}]E_0(\bar{z})/(2m\Omega^2) \tag{2.12}$$

which may also be written

$$(1/e)F(\bar{z}) = -\partial\psi(\bar{z})/\partial\bar{z}, \qquad \psi(\bar{z}) \equiv eE_0{}^2(\bar{z})/(4m\Omega^2), \tag{2.13}$$

introducing the electric pseudopotential $\psi(z)$. This result can be generalized (Kapitsa, 1951; Gaponov and Miller, 1958; Landau and Lifschitz, 1960; Weibel and Clark, 1961):

$$\bar{F}(\bar{x}, \bar{y}, \bar{z}) = -e \operatorname{grad} \psi(\bar{x}, \bar{y}, \bar{z}), \qquad \psi \equiv [e/(4m\Omega^2)]E_0{}^2(\bar{x}, \bar{y}, \bar{z}), \tag{2.14}$$

$\bar{x}, \bar{y}, \bar{z}$ denoting the coordinates of the guiding center of the three-dimensional particle motion. We now remove the balancing force compensating $\bar{F}(\bar{z})$ and allow the guiding center to move. It is plausible that expressions (2.11) to (2.13) remain valid as long as the quasi-stationary behavior condition

$$|\dot{\bar{z}}| \ll \zeta_0\Omega \tag{2.15}$$

is satisfied. In order to check if this condition can be relaxed, we investigate the case of moderately large, constant $\dot{\bar{z}}$ so that over a period $2\pi/\Omega$ the derivative $\partial E_0(\bar{z})/\partial\bar{z}$ may be considered as constant,

$$|[\partial^2 E_0(\bar{z})/\partial^2\bar{z}](2\pi\dot{\bar{z}}/\Omega)| \ll |\partial E_0(\bar{z})/\partial\bar{z}|. \tag{2.16}$$

We use a solution of (2.9) in the form $z = \bar{z} + \dot{\bar{z}}t + \zeta$ and write

$$(1/e)\bar{F}(\bar{z}) = \frac{\Omega}{2\pi}\int_{t=-\pi/\Omega}^{t=+\pi/\Omega} dt\,[E_0(\bar{z}) + (\dot{\bar{z}}t + \zeta)\partial E_0(\bar{z})/\partial\bar{z}] \cos\Omega t. \tag{2.17}$$

Inspection shows that in addition to the terms in (2.11), a term proportional to $\langle\dot{\bar{z}}t\cos\Omega t\rangle_{av}$ appears. For suitably chosen end points of the interval $2\pi/\Omega$ this term vanishes too, leaving the expression for force and pseudopotential unchanged. Again it is plausible that a slow variation of $\dot{\bar{z}}$, $|2\pi\ddot{\bar{z}}/\Omega| \ll |\dot{\bar{z}}|$, may be tolerated. Evaluating the kinetic energy $W(z)$ averaged over one period gives

$$\begin{aligned}\langle W(z)\rangle_{av} \equiv \bar{W} &= \langle(m/2)\dot{z}^2\rangle_{av} \\ &= (m/2)\dot{\bar{z}}^2 + \langle(m/2)\dot{\zeta}^2\rangle_{av} + \langle m\dot{\bar{z}}\dot{\zeta}\rangle_{av}.\end{aligned} \tag{2.18}$$

In the limit, $\Omega \to \infty$, of interest here the last term vanishes because either (2.15) or (2.16) applies for a bound particle. The kinetic energy in the micromotion,

$$\langle(m/2)\dot{\zeta}^2\rangle_{av} = [e^2/(4m\Omega^2)]E_0{}^2(\bar{z}) = e\psi(\bar{z}), \tag{2.19}$$

turns out to be the pseudopotential energy $e\psi$ previously introduced. Consequently, $\bar{W}$ is a constant of the secular motion corresponding to the total energy in systems with time-independent conservative forces and will be referred to as "the energy $\bar{W}$" from here on. The total instantaneous kinetic energy $W(z)$ on the other hand does fluctuate widely,

$$0 \le W(z) \le 2\bar{W}. \tag{2.20}$$

2.4. Single Ion Motion in Quadrupole rf Trap

As an application of (2.14) we consider the same potential as for the Penning trap, Eq. (2.3), but we set

$$A = A_0 \cos\Omega t. \tag{2.21}$$

The electric field has the components

$$-\partial\phi/\partial x = -2Ax, \qquad -\partial\phi/\partial y = -2Ay, \qquad -\partial\phi/\partial z = 4Az. \tag{2.22}$$

Accordingly, the resulting three-dimensional elliptic potential well is given by

$$\psi(\bar{x}, \bar{y}, \bar{z}) = \bar{D}[\bar{x}^2 + \bar{y}^2 + 4\bar{z}^2]/(4z_0{}^2), \qquad \bar{D}/(4z_0{}^2) \equiv eA_0{}^2/(m\Omega^2), \tag{2.23}$$

$\bar{D}$ denoting the depth of the pseudopotential well in the z direction. As is well known, the motion of a particle in such a well is a superposition of three independent harmonic oscillations, along the x and y axes with frequencies $\bar{\omega}_r$ and along the z axis with frequency $\bar{\omega}_z$, explicitly, $\bar{\omega}_z = 2\bar{\omega}_r$. Restricting us to motion purely along the z axis, we expect the z-motion of the guiding center to be described by, γ a phase constant,

$$\bar{z} = \bar{z}_0 \cos(\bar{\omega}_z t + \gamma), \qquad e\bar{D} = mz_0{}^2\bar{\omega}_z{}^2/2, \tag{2.24}$$

and the complete motion by

$$z = \bar{z} - \zeta_0 \cos\Omega t. \tag{2.25}$$

Without serious lack of generality $\gamma = 0$ may be assumed in the following. With $E_0(\bar{z}) = -4A_0\bar{z}$ from (2.3), Eq. (2.25) may be written

$$z = [1 + (\sqrt{2}\bar{\omega}_z/\Omega)\cos\Omega t]\bar{z}_0 \cos\bar{\omega}_z t. \tag{2.26}$$

The pseudopotential approach is justified because in the region $z \simeq 0$ condition (2.16) applies, and in the region $z \simeq \bar{z}_0$ condition (2.15) applies. Provided the "stability parameter" $\Omega/\bar{\omega}_z$ is large compared to unity, it can also be shown by direct substitution that in this limit (2.26) is a solution of the Mathieu differential equation associated with the rigorous treatment of the problem (Paul *et al.*, 1958; Fischer, 1959). Multiplying (2.26) out, terms proportional to $\cos\bar{\omega}_z t$ and $\cos\bar{\omega}_z t\cos\Omega t$ occur. The last one may be decomposed to

$$\cos(\Omega + \bar{\omega}_z)t + \cos(\Omega - \bar{\omega}_z)t. \tag{2.27}$$

This shows that the motion contains spectral components at $\bar{\omega}_z$ and $\Omega \pm \bar{\omega}_z$. The rigorous solution for finite values of $\Omega/\bar{\omega}_z$ also contains components at

$$s\Omega \pm \bar{\omega}_z, \qquad s = 2, 3, 4, \ldots, \infty.$$

It is now interesting to compare $\bar{\omega}_z$ with ω_z for operation of the same trap in the Penning mode with $A = A_0$. We may write (for a negative ion) using (2.3) and (2.23)

$$\bar{\omega}_z^2/\omega_z^2 = \bar{D}/D = \tfrac{1}{2}\omega_z^2/\Omega^2 \tag{2.28}$$

or

$$\sqrt{2}\,\bar{\omega}_z\,\Omega = \omega_z^2, \qquad \bar{D}/D = 2^{-1/2}\bar{\omega}_z/\Omega. \tag{2.29}$$

We see that for any specific geometry (e.g., as given in Fig. 1) operation at $U = V_0 \cos \Omega t$ leads to an effective well depth in the z direction which is by the factor $2^{-1/2}\bar{\omega}_z/\Omega$ smaller than for operation at $U = U_0 = V_0$. Since U_0 is related to D by (2.3) we may write

$$V_0 = \sqrt{2}\,[1 + \tfrac{1}{2}(r_0/z_0)^2](\Omega/\bar{\omega}_z)\,\bar{D}. \tag{2.30}$$

These results have been obtained in the limit $\Omega/\bar{\omega}_z \gg 1$. The question as to how far this restriction may be relaxed arises. It is found (Paul *et al.*, 1958; Wuerker *et al.*, 1959) that trapping can be achieved down to $\Omega > 2\bar{\omega}_z$. For $\Omega \leq 2\bar{\omega}_z$, a rapidly growing instability similar to parametric excitation (Landau and Lifschitz, 1960) occurs. Similar instabilities are observed when Ω coincides with certain higher order (Busch and Paul, 1961) harmonic combinations of $\bar{\omega}_z$ and $\bar{\omega}_r$ and the rf field is sufficiently inhomogeneous of a related order. It is a general property of a harmonic oscillator to respond to a harmonically related inhomogeneous alternating force field. Because small contributions from higher order multipole fields cannot be avoided in a practical trap it seems advisable to make the stability parameter $\Omega/\bar{\omega}_z$ large as the contributions from such fields may be expected to be the weaker the higher their order. Avoiding integer ratios we have found values $\Omega/\omega_z \simeq 10$ satisfactory. Choosing size, depth, shape, and stability parameter of a trap determines the operating voltage by (2.30). The frequency $\bar{\omega}_z$ and therefore Ω are then determined by the energy relation (2.24), $(m/2)(z_0^2\,\bar{\omega}_z^2) = e\bar{D}$. Once z_0, r_0, $\bar{\omega}_z$, and Ω have been fixed for a given apparatus it is also of interest to know at which values of V_0 other ion masses will come into resonance. We note that under these conditions, according to (2.24), it follows that

$$\bar{D} \propto m \tag{2.31}$$

and with (2.30), we have

$$V_0(m) \propto m \tag{2.32}$$

indicating proportionality between ion mass and rf voltage necessary to cause oscillation at $\bar{\omega}_z$. In other experimental situations we wish to know at what frequencies other ions will oscillate in a given trap for fixed Ω and V_0 and what their well depth will be. Here we find from (2.30) the relation $\bar{D}/\bar{\omega}_z = \text{const}$, which with (2.24) gives

$$\bar{\omega}_z \propto 1/m \qquad \text{and} \qquad \bar{D} \propto 1/m. \tag{2.33}$$

This demonstrates the difficulties encountered when attempting to trap ions of very different masses simultaneously.

2.5. Ion Cloud in Temperature Equilibrium

The motion of the stored ions is of course three dimensional. Contemplating extended storage it seems reasonable to allow for cumulative effects of small conservative interactions due to various causes which, while leaving $\bar{W}$ constant, may still change the character of the ion orbit. By making the well depth in the axial and the radial directions the same, $\bar{D} \equiv \bar{D}_z = \bar{D}_r$, we avoid the possibility that an ion initially carrying out a large amplitude oscillation in, for example, the z direction will later hit the ring electrode, as would be the case for $\bar{D}_r < \bar{D}$. Inspection of (2.33) shows that equal depths result for $r_0 = 2z_0$. We also note that $\bar{\omega}_z = 2\bar{\omega}_r$. By adding a dc component U_0 to U, $U = U_0 + V_0 \cos \Omega t$, the potential due to U_0 alone simply adds to ψ as given in (2.23). This is to be expected since, in our limiting case $\bar{\omega}_z \ll \Omega$, the small amplitude micromotion responsible for the trapping force is not affected by the presence of the weak dc field. Judicious choice of U_0 provides another means of symmetrizing a general well, $r_0 \neq 2z_0$. In both cases it is reasonable to define as the active trap volume an ellipsoid of rotation closely fitting into the electrode structure,

$$V_t = \tfrac{4}{3}\pi z_0\, r_0^2. \tag{2.34}$$

As our next task we attempt to estimate the storage capacity of the zero dc trap, with $r_0 = 2z_0$. Filling it with a number of ions at rest (except for the micromotion) we would expect that the electrostatically interacting ions would arrange themselves in such a fashion at the bottom of the well that a test ion would experience no force; that is, we would expect a flat net potential in the ellipsoidal ion-filled region,

$$\psi + \phi_i = \text{const}, \tag{2.35}$$

where ϕ_i denotes the electrostatic potential due to the ions. Taking the Laplacian on both sides, we have

$$-\Delta\phi_i = \Delta\psi = 4\pi\rho_{\max}, \qquad \rho_{\max} = 3\bar{D}/(4\pi z_0^2) = en_{\max}, \tag{2.36}$$

indicating a constant charge density. Expression (2.36) may be used to obtain the distance between the stationary ions r_{min}, which here equals that of closest approach,

$$r_{min}^3 = 4\pi e z_0^2/(3\bar{D}) = 1/n_{max}, \tag{2.37}$$

$$n_{max} = 1.66 \times 10^6 \bar{D}/z_0^2, \qquad [z_0] = \text{cm}, \quad [\bar{D}] = \text{volt}.$$

In a numerical example we find, for singly charged ions and for $e = 4.8 \times 10^{-10}$ cgs, $z_0 = 2.5$ cm, and $D = 6.2$ volts $\simeq 1/50$ cgs, the value $r_{min} = 0.84 \times 10^{-2}$ cm, demonstrating the excellent isolation between the ions. At room temperature this would decrease to $r_{min} = 2 \times 10^{-6}$ cm, as evaluated from

$$r_{min} = e^2/3k\mathrm{T}_i. \tag{2.38}$$

Even at this value the average overlap of the electronic wave functions would be orders of magnitude smaller than for a neutral gas of the same density. After this digression we return to the original question of storage capacity. From (2.34) and (2.36) we get, for the maximum storable charge q_{max} and the maximum total ion number N_{max},

$$N_{max} e \equiv q_{max} = 4\bar{D}z_0; \tag{2.39}$$

$$N_{max} = 2.8 \times 10^7 \bar{D} z_0, \qquad [\bar{D}] = \text{volt}, \quad [z_0] = \text{cm}.$$

The important question, if the supposed zero secular motion ion configuration would be stable in actuality, has so far not been discussed. The synchronous breathing of the ion cloud at the frequency Ω only modifies the rf field in the trap by a constant factor very close to unity. Ion-ion collisions will of course occur in a cloud of ions at the finite temperature T_i, $3K\mathrm{T}_i = \langle W \rangle_{av}$. As the appropriate collision interval we take in an approximation that given in the literature for a uniform plasma (Spitzer, 1956; McDonald *et al.*, 1957):

$$t_c = 0.78 \times 10^7 A^{1/2} (k\mathrm{T}_i/e)^{3/2} n^{-1} Z^{-4} (\ln \Lambda)^{-1}, \tag{2.40}$$

$$[t_c] = \text{sec}, \qquad [k\mathrm{T}_i/e] = \text{volt},$$

where A and Z are atomic weight and ionic charge and where $\Lambda = r_{max}/r_{min}$ is the ratio of the cutoff distance for Coulomb interaction of an ion with its neighbors to that of closest approach. Since the choice of r_{max} is not very critical it seems reasonable to set $r_{max} \simeq z_0$ which gives $\ln \Lambda \simeq 20$ in the region of interest. A numerical estimate for ions at room temperature and density $n = n_{max}$ from (2.37) with $D = 6$ volts and $z_0 = 2.5$ cm, gives for protons, $A = Z = 1$, $t_c = 1$ msec, showing that such collisions can be quite important.

However, at least for the case of a cloud of identical ions in a homogeneous rf field, these collisions cannot lead to energy absorption from the field. Here the rf field simply causes the center of mass of the cloud of ions to oscillate with amplitude ζ_0 [see (2.10)] while the individual ions in the center-of-mass frame carry out their random rectilinear motions. Since ion-ion collisions cannot transform energy of the motion of the center of mass into kinetic energy of the relative motion of the ions, no energy absorption from the field can take place. This is not strictly true anymore in an inhomogeneous rf field; e.g., hard spheres of a radius which is an appreciable fraction of z_0 and bearing a charge at the center when moving along the z axis of a quadrupole trap undergoing head-on collisions will absorb energy from the rf field. Assuming that analogous long-range effects are unimportant in an ion trap we expect that in a perfect vacuum and in a trap geometrically and electrically perfect a cloud of identical ions would not be subject to any rf heating. Consequently, we propose to treat the ion cloud as if it were contained in an ordinary three-dimensional harmonic oscillator potential. Because of the long available experimental storage times, $T \gg t_c$, the ions may be considered to be in thermal equilibrium with themselves and assigned a temperature T_i. When cold ions $k\mathrm{T}_i \ll e\bar{D}_q$ of total charge $q < q_{max}$ are confined in a trap, they fill it up to a level $\bar{D}_q$ like a fluid occupying at constant density n_{max} an ellipsoidal region with half-axes z_q, $r_q = 2z_q$, $(z_q/z_0)^2 = \bar{D}_q/\bar{D}$ and volume $V_q = (16/3)z_q^3$. For the "fluid" level $\bar{D}_q$ the relation

$$(\bar{D}_q/\bar{D})^3 = (q/q_{max})^2 \tag{2.41}$$

holds. If the temperature rises the ion cloud expands, and its boundaries wash out. Also, loss of ions due to collisions of the Boltzmann tail, $W > e\bar{D}$, with the electrodes becomes important. A self-collision parameter T_c^* for the trap may be defined as the t_c from (2.40) for $3k\mathrm{T}_i = e\bar{D}$ and $n = n_{max}$ taking $Z = 1$,

$$T_c^* \equiv 0.046 z_0^2 \bar{D}^{1/2} A^{1/2}, \qquad [z_0] = \text{cm}, \quad [\bar{D}] = \text{volt}. \tag{2.42}$$

For ions only partially filling a trap, as will always be assumed now, $q \ll q_{max}$, at the temperature $3k\mathrm{T}_i = e\bar{D}$, where every ion-ion collision may be expected to lead to loss at the electrodes,

$$T_c \equiv (q_{max}/q) T_c^* \tag{2.43}$$

may be interpreted as the (hot) ion lifetime. In the intermediate region $0 < 3k\mathrm{T}_i < e\bar{D}$, we approximate the ion density of the ion cloud roughly extending over an ellipsoidal region with half-axes z_{qT}, r_{qT} by

$$n \simeq n_{max}[e\bar{D}_q/(e\bar{D}_q + 3k\mathrm{T}_i)]^{3/2} \tag{2.44}$$

$$(z_{qT}/z_0)^2 \simeq (e\bar{D}_q + 3k\mathrm{T}_i)/(e\bar{D}).$$

For the average energy $3k\mathrm{T}_i \gg e\bar{D}_q$, we use this to obtain a convenient expression for the self-collision time

$$t_c \simeq (3k\mathrm{T}_i/e\bar{D})^3 T_c. \tag{2.45}$$

At very low temperatures, $3k\mathrm{T}_i \ll e\bar{D}_q$, t_c becomes independent of q, as seen from (2.37) and (2.40),

$$t_c \simeq 0.24A^{1/2}(k\mathrm{T}_i/e)^{3/2}\mathrm{z}_0^2/\bar{D}, \quad [\mathrm{z}_0] = \mathrm{cm}, \quad [k\mathrm{T}_i/e] = [\bar{D}] = \mathrm{volt}. \tag{2.46}$$

We now attempt to obtain an expression for the rate of ion loss at the electrodes in the intermediate temperature region by a detailed balancing argument. For a parabolic well extending far beyond z_0, r_0, the fraction f_B of the N ions in the well with $W \geq e\bar{D}$, where $\bar{D}$ is now much less than its depth, in temperature equilibrium is

$$f_B \simeq \tfrac{1}{2}(e\bar{D}/k\mathrm{T}_i)^2 \exp(-e\bar{D}/k\mathrm{T}_i). \tag{2.47}$$

An ion in this Boltzmann distribution tail undergoes collisions with the majority of energies around $3k\mathrm{T}_i$ and thereby returns to the majority at a rate roughly equal to T_c^{-1} as defined in (2.43). On the other hand, tail ions are created from the majority at the rate NT_B^{-1}. At equilibrium this rate must be given by

$$NT_B^{-1} \simeq f_B NT_c^{-1} \tag{2.48}$$

or

$$T_B \simeq 2T_c(k\mathrm{T}_i/e\bar{D})^2 \exp(e\bar{D}/k\mathrm{T}_i).$$

For the loss rate of fast ions in our trap of depth $\bar{D}$, we now take the creation rate T_B^{-1} of tail ions just developed. Simultaneously, the loss of energetic ions results in a heat loss of the ion cloud

$$d(3k\mathrm{T}_i/e)/dt \simeq -\bar{D}/T_B, \tag{2.49}$$

which already in time intervals short compared to T_B can be appreciable on a percentage basis. The equilibrium temperature established will be that at which the heat input due to various dissipative mechanisms balances the heat loss of the ion cloud. By using the experimental ion lifetime T in place of T_B, Eq. (2.48) may be used to establish an upper limit for the equilibrium temperature of the cloud for the region $e\bar{D}/3k\mathrm{T}_i > 2$:

$$(e\bar{D}/3k\mathrm{T}_i) \gtrsim \tfrac{1}{3}\ln(T/T_c) + \tfrac{2}{3}\ln[0.1\ln(T/T_c)] + 1.3. \tag{2.50}$$

In a numerical example with $T = 600$ sec, $\mathrm{z}_0 = 0.16$ cm, and $q_{max}/q = 30$, which is similar to analogous experimentally realized conditions, one would find $e\bar{D}/3k\mathrm{T}_i \gtrsim 4.3$ for $[\mathrm{He}^3]^+$ in a trap of depth $\bar{D} = 6$ volts.

2.6. Collision Heating

We now turn to specific dissipative mechanisms such as rf heating of the stored ion cloud due to the presence of other atoms and ions in the trap region. As a model of these processes occurring at intervals T_r, we choose first purely elastic, totally randomizing collisions of ions in a homogeneous rf field with a "forest" of uniformly distributed fixed scattering centers. The center of mass of an ensemble of ions, all of which have just undergone a collision with a center near $\bar{z}$, will then be at rest at the instant t_1. Interaction with the electric rf field will, according to (2.9) and (2.10), cause the center of mass to move with a translational velocity $\dot{\bar{z}} = -\dot{\zeta}(t_1)$, on which of course the micromotion velocity $\dot{\zeta}$ is superposed. The average total energy per ion of the center-of-mass motion, that is available for degradation into heat of amount ΔW in subsequent randomizing collisions, is, consequently,

$$\Delta W = 2(m/2)\langle\dot{\zeta}^2\rangle_{av} = 2e\psi(\bar{z}). \tag{2.51}$$

If this is further averaged over the secular oscillation, assuming a constant rate of collisions, we have

$$\Delta W = W_i, \tag{2.52}$$

where W_i is the initial ion energy. The generality of this result is not affected by focusing on scattering centers located near the z axis. Reasonably heavy atoms and other ions of mass m_r may be expected to cause similar strong heating though reduced by a factor $a(m/m_r) \lesssim 1$, which may also depend on other variables. The corresponding heat input to the ion cloud is then

$$\partial(3k\mathrm{T}_i)/\partial t = a(m/m_r)\, 3k\mathrm{T}_i/T_r. \tag{2.53}$$

Conversely, collisions with much lighter cold partners, which essentially create viscous drag, result in a lowering of the average total ion energy implying a negative a. In this limit the micromotion is not interrupted by the collisions but only slightly modified in phase and amplitude, while any secular motion gradually damps out exponentially. This effect was first demonstrated for metal particles in air (Wuerker *et al.*, 1959) and later for Hg^+ in helium gas at about 10^{-5} Torr (Huggett and Menasian, 1965). In order to shine some light on the interesting question at which value m/m_r the factor $a(m/m_r)$ vanishes, as the above suggests, we now discuss collisions with scattering centers of mass $m_r = m$ which are initially at rest, restricting us to head-on collisions. Immediately after such a collision an ion of initial energy W_i will be at rest, and the subsequent average energy absorption from the rf field will again be W_i, as described by formulas (2.51) and (2.52), corresponding to zero net energy gain during the collision. This may be taken to indicate that for general, not only head-on, collisions

$$|a(1)| \ll 1. \tag{2.54}$$

The same formulas (2.51) and (2.52) may be applied in even better approximation now to the important case of collisions with parent gas atoms. Here resonant charge exchange dominates by about an order of magnitude over momentum transfer. The ions, having been formed by fast ions passing on their charge to thermal atoms, may, independent of the collision parameter, be assumed to be initially at rest in good approximation. By the same argument as given before no energy input into the self-regenerating ion cloud occurs due to the collision process. A constant collision rate has been assumed everywhere. This is a fair approximation in general since the *average* instantaneous total kinetic energy is a constant of the motion and according to (2.18) equal to $\bar{W}$. In the region of orbiting collisions the assumption is even rigorous [see (2.1)]. However, at higher relative velocities, about 10^6 cm/sec, the charge-exchange rate T_{ce}^{-1} becomes roughly velocity-proportional (Rapp and Francis, 1962). Now, from ions of initial oscillation amplitudes $\bar{z}_0$, zero velocity ones are preferentially created when $\dot{z}$ is largest, $\dot{z}_{max} = \dot{\zeta}_{max} = \sqrt{2}\dot{z}_{max}$, which is in the $\bar{z} \simeq \bar{z}_0$ region whereby, in accordance with the expression (2.51), net energy absorption results and the factor a consequently assumes a small positive value. By taking $T_r = T_{ce}$ in (2.53) and using the above a value we obtain the appropriate rate of heat input. Charge exchange with other atomic species leads of course to immediate loss of the ion of interest. When predominant, the heating processes sketched before eventually cause the ions to be lost at the electrodes.

2.7. Ion Creation

The principal way in which traps have been filled has been electron bombardment of background gas. It is essential here to realize that the maximum current density of electrons at energy eU_e that can flow through the space between two highly transparent grids at equal potential separated by a distance d is limited to

$$j_{e,max} = 1.9 \times 10^{-5} U^{3/2}/d^2, \qquad (2.55)$$

$$[j_{e,max}] = \text{amp/cm}^2, \quad [U_e] = \text{volt}, \quad [d] = \text{cm},$$

provided no virtual cathode is to appear (Rothe and Kleen, 1951). In the axially symmetric design it is not practical to make the beam cross section larger than about d^2, resulting in a maximum electron current available of

$$i_{e,max} \simeq 2 \times 10^{-5} U^{3/2}, \quad [i_{e,max}] = \text{amp}. \qquad (2.56)$$

This is of course only a rough estimate since (2.55) is not strictly applicable to the complex trap structure. The total electron charge q_e necessary to produce an ion charge q_{max} also does not depend on the trap size z_0,

$$q_e \simeq 2.2 \times 10^{-12} \bar{D}/(n_r Q_i), \quad [q_e] = \text{coulomb}, \quad [\bar{D}] = \text{volt}. \qquad (2.57)$$

Here Q_i and n_r are ionization cross section and density of the atomic species to be ionized. Such q_e values can usually be realized within milliseconds. At ultrahigh vacuums it is of course still possible to pulse the gas pressure or even use pulsed atomic beams. The release of bursts of adsorbed parent gas from metal electrodes under electron bombardment acts in a similar way. An experimental value for the stored fractional charge q/q_{max} or filling factor may be obtained by measuring the dc bias voltage necessary to restore the oscillation frequency of a small sample of indicator ions, of a mass not too different from that of those under study, to its old value after it has been shifted by the space-charge potential of the ion sample of interest of total charge q. Assuming constant ion density over the whole trap, we have from (2.36) that

$$q/q_{max} = \Delta\bar{D}/\bar{D}, \qquad (2.58)$$

where $\Delta\bar{D}$ is the well-depth change corresponding to the compensating dc voltage applied. Of course, V_0 has been adjusted to bring the indicator ions into resonance. Ideally, V_0 should be held constant in this measurement. However, if some change of V_0 can be tolerated subsequent to filling of the trap, the constant $\bar{\omega}_z$ operation assumed here is much more convenient experimentally. Because of the averaging effect of the indicator ion motion, this procedure should give good approximate values even for inhomogeneous ion distributions, when large oscillation amplitudes of the indicator ions are used.

2.8. Sample Trap Data

In conclusion, as an illustration of the various points raised in the preceding discussion, we describe the trap used in Major's experiments in numerical detail. Its relevant parameters are listed in Table II and a scale drawing of its mechanical construction is shown in Fig. 3. The trap depth was derived from

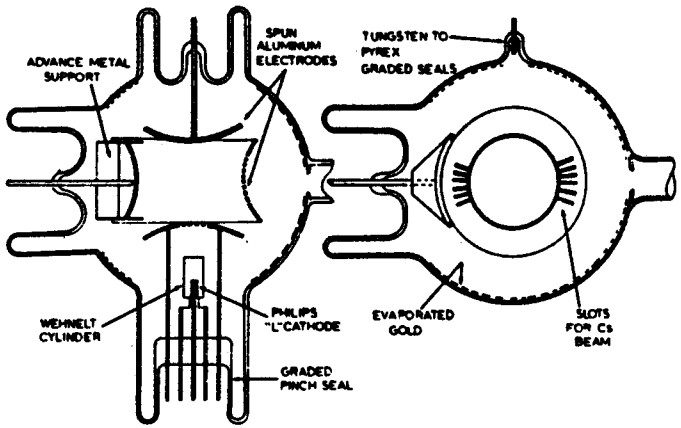

FIG. 3. Scale drawing of illustrative rf quadrupole trap described in Table II.

TABLE II

DIMENSIONS, OPERATING PARAMETERS, OBSERVED AND DERIVED ION DATA FOR ILLUSTRATIVE TRAP

Axial dimension:	$z_0 = 2.5$ cm
Radial dimension:	$r_0 = 3.5$ cm
Effective trap volume:	$V_t = 128$ cm^3
dc bias:	$U_0 = 7$ volt
ac drive amplitude:	$V_0 = 175$ volts
Frequency:	$\Omega = 2\pi \times 1$ MHz
Vacuum:	$p \simeq 3 \times 10^{-8}$ Torr
Background:	Mostly He^4
Electron current:	$i_e = 1$ mA
Electron acceleration voltage:	$U_e = 400$ volts
Electron pulse duration:	~ 0.1 sec
Ionic species:	$[He^4]^+$
Axial oscillation frequency:	$\bar{\omega}_z = 2\pi \times 110$ kHz
Maximum velocity in trap center:	$z_0\bar{\omega}_z = 1.73 \times 10^6$cm/sec
Axial depth:	$\bar{D} = 6.2$ volts
Radial depth:	$\bar{D}_r = 8.2$ volts
Maximum instantaneous energy:	$W_{max} \simeq 12.4$ eV
Maximum experimental stored charge:	$q \simeq 10^7 e$
Maximum charge:	$q_{max} \simeq 3 \times 10^8 e$
Ion lifetime: (maximum attained):	$T = 8$ sec $T = 50$ sec
Self-collision parameter:	$T_c^* = 1.5$ sec
He^+–He charge exchange:	$T_{ce} \simeq 0.3$ sec

relation (2.24), which applies also in the presence of a dc bias, as $\bar{D} = 6.2$ volts. Since $r_0/z_0 \simeq \sqrt{2}$ the dc bias voltage $U_0 = 7$ volts contributed -3.5 volts to $\bar{D} = \bar{D}_z$. Therefore, we have $\bar{D}_z$ (ac only) $= 9.7$ volts and $\bar{D}_r$ (ac only) $= 4.9$ volts giving $\bar{D}_r = 8.4$ volts. In order to check Eq. (2.30), we evaluate $\bar{\omega}_z$(ac only) $= 2\pi \times 138$ kHz using the relation

$$\bar{\omega}_z \text{ (ac only)}/\bar{\omega}_z = [\bar{D}_z \text{ (ac only)}/\bar{D}]^{1/2}$$

and obtain $V_0 = 200$ volts, in only fair agreement with the experimental value. The electron acceleration voltage was chosen as $U_e \simeq 2V_0$ in a compromise effort to retain reasonably straight electron trajectories inside the trap, in the face of the electron space-charge potential depression and the strong rf fields

there, without causing excessive heating of the electrode structure The electron current was pulsed by applying a positive voltage pulse, +45 volts with respect to the cathode, to the Wehnelt cylinder, ordinarily held at a small negative voltage. Comparison of the experimental lifetimes $T = 8$ sec and $T = 50$ sec (the latter attained at best vacuum, background not analyzed) with the hot ion self-collision time $T_c \simeq 50$ sec defined in (2.43) shows that ion-ion collisions are not very important for this trap and that the average ion energy must be near $e\bar{D}$. We attribute the ion loss primarily to the repeated small energy increments furnished by charge-exchange collisions with the parent gas according to the arguments presented, which suggest a small positive a and which are in agreement with the experimental observation that about $T/T_{ce} \simeq 30$ such collisions are necessary to drive an ion against an electrode. The maximum charge density in a symmetrized $r_0/z_0 = \sqrt{2}$ trap is, for equal $\bar{D}$ and z_0, given by $n_{s,max} = \frac{4}{3}n_{max}$. Applying this to the Major trap gives $n_{s,max} \simeq 2.2 \times 10^6/\text{cm}^3$, and with the listed volume $q_{max} \simeq 2.8 \times 10^8 e$. The maximally storable experimental charge listed was determined for a $(He^3)^+$ sample according to the procedure leading to Eq. (2.58), using H_2^+ created from the background gas as the test ions. Application of a dc voltage of -0.3 volt compensating the $(He^3)^+$ space charge was required. With $\bar{D}(He^3) = \frac{3}{4}\bar{D}(He^4) = 4.6$ volts this is equivalent to a filling factor $q/q_{max} \simeq 1/30$.

Besides the axially symmetric quadrupole trap discussed here, other configurations have also been operated successfully. These include circular traps for electrons and ions simultaneously contained by the electronic space charge (Drees and Paul, 1964), circular (Church, 1966) and race-track-shaped traps for hydrogen and helium ions (Church, 1965) and for mercury ions (Huggett and Menasian, 1965), all obtained by bending a 4-wire mass filter structure (Paul and Steinwedel, 1953) into these shapes, and also a cubic trap (Wuerker *et al.*, 1959). In the circular trap, lifetimes of 600 sec were observed for He^+ ions at a background pressure of 3×10^{-10} Torr of helium. It had a depth $\bar{D} = 6$ volts and separation between electrodes was $2x_0 = 3.2$ mm. Much shorter self-collision times t_c obtain here than in the Major trap. Using in a rough approximation Eqs. (2.42), (2.43), and (2.45) developed for the axially symmetric configuration, setting $z_0 = x_0$, and assuming $q_{max}/q = 30$, we find $T_c^* = 6$ msec, $T_c = 200$ msec, and $t_c = 3$ msec. Comparable t_c values have been experimentally observed for room temperature electrons stored in the Penning trap (described earlier), to which system much of our analysis is applicable. By observing the delayed temperature increase in the z motion following pulse heating of the cyclotron motion in the x–y plane we have estimated (Walls, 1966) $t_c \lesssim 5$ msec. All this demonstrates the importance of the concept of a stored ion cloud in thermodynamical equilibrium with itself in future experiments.

REFERENCES

Balling, L. C., and Pipkin, F. M. (1965). *Phys. Rev.* **139**, A19.
Busch, F. V., and Paul, W. (1961). *Z. Physik* **164**, 588.
Church, D. (1965). Private communication.
Church, D. (1966). Private communication.
Dehmelt, H. G. (1956a). *Phys. Rev.* **103**, 1125.
Dehmelt, H. G. (1956b). Optical Pumping Symposium, 123rd AAAS Meeting, New York, Dec. 26, 1956.
Dehmelt, H. G. (1958a). *Phys. Rev.* **109**, 381.
Dehmelt, H. G. (1958b). *J. Phys. Radium* **19**, 866.
Dehmelt, H. G. (1961). Unpublished.
Dehmelt, H. G. (1962). *Bull. Am. Phys. Soc.* **7**, 470.
Dehmelt, H. G. (1963). *Bull. Am. Phys. Soc.* **8**, 23.
Dehmelt, H. G., and Jefferts, K. B. (1962). *Phys. Rev.* **125**, 1318.
Dehmelt, H. G., and Major, F. G. (1962). *Phys. Rev. Letters* **8**, 213.
Dicke, R. H. (1953). *Phys. Rev.* **89**, 472.
Drees, T., and Paul, W. (1964). *Z. Physik* **180**, 340.
Fischer, E. (1959). *Z. Physik* **156**, 1.
Fortson, E. N., Major, F. G., and Dehmelt, H. G. (1966). *Phys. Rev. Letters* **16**, 221.
Gaponov, A. V., and Miller, M. A. (1958). *Zh. Eksperim. i Teor. Fiz.* **34**, 242.
Huggett, G. R., and Menasian, S. (1965). Private communication.
Jefferts, K. B. (1962). Thesis, University of Washington, University Microfilms, Ann Arbor, Michigan.
Kapitsa, P. L. (1951). *Zh. Eksperim. i Teor. Fiz.* **21**, 588.
Landau, L. D., and Lifschitz, E. M. (1960). "Mechanics." Pergamon, Oxford.
Major, F. G. (1962). Thesis, University of Washington, University Microfilms, Ann Arbor, Michigan.
Major, F. G., and Dehmelt, H. G. (1967). *Phys. Rev.* To be published.
McDonald, W. M., Rosenbluth, M. N., and Chuck, W. (1957). *Phys. Rev.* **107**, 350.
Paul, W., Osberghaus, O., and Fischer, E. (1958). *Forschungsber. Wirtsch. Verkehrsministeriums Nordrhein-Westfalen* No. 415.
Paul, W., and Steinwedel, H. (1953). *Z. Naturforsch.* **8a**, 448.
Penning, F. M. (1936). *Physica* **3**, 873.
Pierce, T. R. (1949). "Theory and Design of Electron Beams," Chap. 3. Van Nostrand, Princeton, New Jersey.
Rapp, D., and Francis, W. E. (1962). *J. Chem. Phys.* **37**, 2631.
Richardson, C. B., Jefferts, K. B., and Dehmelt, H. G. (1967). *Phys. Rev.* To be published.
Rothe, H., and Kleen, W. (1951). "Grundlagen und Kennlinien der Elektronenröhren," Ch. 6. Akademische Verlagsgesellschaft, Leipzig.
Spitzer, L. (1956). "Physics of Fully Ionized Gases." Wiley (Interscience), New York.
Stevenson, D. P., and Gioumousis, G. (1958). *J. Chem. Phys.* **29**, 294.
Walls, F. (1966). Private communication.
Weibel, E. S., and Clark, G. L. (1961) *Plasma Phys.* **2**, 112.
Wuerker, R. F., Goldenberg, H. M., and Langmuir, R. V. (1959). *J. Appl. Phys.* **30**, 441.

OPTICAL PUMPING METHODS IN ATOMIC SPECTROSCOPY

B. BUDICK

The Hebrew University
Jerusalem, Israel

I. Introduction

Experimental techniques that involve the use of optical pumping have been applied to a wide variety of phenomena. The earlier work was primarily concerned with lifetimes of excited states and with the effect of collisions in producing broadening, shifts, and asymmetries in spectral lines [1]. Resonance fluorescence from an atomic beam is still used for high-resolution optical spectroscopy as a means of reducing the Doppler width [2].

Procedures utilizing magnetic resonance are clearly more suited for precision work. Radio-frequency spectroscopy of excited atomic states was first suggested by Bitter [3] and by Brossel and Kastler [4]. The natural lifetime of the excited state is in principle the only limit on the precision of such an experiment. With the extension of the technique to ground states, linewidths comparable to atomic-beam magnetic-resonance experiments have been obtained. All optical pumping experiments utilizing magnetic resonance have in common the achievement of a population inequality in the ground and/or excited state. This inequality is partially or completely eliminated by application of the radio frequency. The population change is detected